

## Research Article

# Effects of Dufour and Modified Forchhemier for Hydromagnetic Free Convective Heat and Mass Transfer Flow along a Permeable Inclined porous Plate with Heat Generation and Thermophoresis

<sup>1</sup>M.J. Uddin and <sup>2</sup>M. Enamul Karim

<sup>1</sup>Department of Natural Science, FSIT, Daffodil International University, Dhaka

<sup>2</sup>Department of Mathematics, Comilla University, Comilla-3500, Bangladesh

**Abstract:** This study presents the numerical simulations to investigate the effects of the magnetic field parameter, Modified Forchhemier number, Prandtl number, Modified Darcy number, the Local Grashof number, the Dufour number and the Schmidt number on steady two-dimensional, laminar, hydromagnetic flow with heat and mass transfer over a semi-infinite, permeable inclined plate in the presence of thermophoresis and heat generation is carefully considered and equipped numerically. A similarity transformation is used to shrink the governing non-linear partial differential equations into ordinary differential equations. The obtained locally similar equations are then solved numerically by applying Nachtsheim-Swigert shooting iteration technique with sixth-order Runge-Kutta integration scheme. Comparisons with previously published study are performed and the results are found to be in very good agreement. Numerical results for the dimensionless velocity, temperature and concentration profiles are reported graphically as well as for the skin-friction coefficient, wall heat transfer and particle deposition rates are investigated for an assortment of values of the parameters inflowing into the problem.

**Keywords:** Free convection, heat generation, hydromagnetic flow, inclined porous plate, mass transfer, temperature and concentration, thermophoresis, velocity

## INTRODUCTION

In recent years, the problems of free convective and heat transfer flows through a porous medium under the influence of a magnetic field have been attracted the attention of a number of researchers because of their possible applications in many branches of science and technology, such as its applications in transportation cooling of re-entry vehicles and rocket boosters, cross-hatching on ablative surfaces and film vaporization in combustion chambers. On the other hand, flow through a porous medium have numerous engineering and geophysical applications, for example, in chemical engineering for filtration and purification process; in agriculture engineering to study the underground water resources; in petroleum technology to study the movement of natural gas, oil and water through the oil reservoirs. In view of these pragmatic applications, many researchers have studied MHD free convective heat and mass transfer flow in a porous medium; some of them are Raptis and Kafoussias (1982) and Kim (2004).

Thermophoresis is the expression describing the fact that small micron sized particles suspended in a non-isothermal gas will acquire a velocity in the direction of decreasing temperature. The gas molecules

coming from the hot side of the particles have a greater velocity than those coming from the cold side. The faster moving molecules collide with the particles more forcefully. This difference in momentum leads to the particle developing a velocity in the direction of the cooler temperature. The magnitudes of the thermophoretic force and velocity are proportional to the temperature gradient and depend on many factors akin to thermal conductivity of aerosol particles and carrier gas. They also depend on the thermophoretic coefficient, the heat capacity of the gas and the Knudsen number. The velocity acquired by the particles is called the thermophoretic velocity and the force experienced by the suspended particles due to the temperature gradient is known as the thermophoretic force. Thermophoresis causes small particles to set down on cold surfaces. The widespread example of this phenomenon is the blackening of glass globe of kerosene lanterns, chimneys and industrial furnace walls by carbon particles. Corrosion of heat exchanger, which reduces heat transfer coefficient and fouling of gas turbine blades are other examples of this phenomenon. Thermophoresis principle is utilized to manufacture graded index silicon dioxide and germanium dioxide optical fiber preforms used in the field of communications. Thermophoretic deposition of

**Corresponding Author:** M. J. Uddin, Department of Natural Science, FSIT, Daffodil International University, Dhaka, Bangladesh

This work is licensed under a Creative Commons Attribution 4.0 International License (URL: <http://creativecommons.org/licenses/by/4.0/>).

radioactive particles is considered to be one of the essential factors causing accidents in nuclear reactors. Maxwell (Kennard, 1938) first investigates the physical process responsible for thermophoresis while explaining the radiometric effect. Goren (1977) studied thermophoresis in laminar flow over a horizontal flat plate. He found the deposition of particles on cold plate and particles free layer thickness in hot plate case. Thermophoresis of particles in a heated boundary layer was studied by Talbot *et al.* (1980). Thermophoresis phenomenon has many pragmatic applications in removing diminutive particles from gas streams, in determining exhaust gas particle trajectories from combustion devices and in studying the particulate material deposition on turbine blades. It has been established that thermophoresis is the foremost mass transfer mechanism in the Modified Chemical Vapor Deposition (MCVD) progression as currently used in the fabrication of optical fiber preforms. Blasius series solution has been sought by Homsy *et al.* (1981). Thermophoresis in natural convection for a cold vertical surface has been studied by Epstein *et al.* (1985). The thermophoretic deposition of the laminar slot jet on an inclined plate for hot, cold and adiabatic plate conditions with viscous dissipation effect were presented by Garg and Jayaraj (1988). Jia *et al.* (1992) studied the interaction between radiation and thermophoresis in forced convection laminar boundary layer flow. Chiou and Cleaver (1996) analyzed the effect of thermophoresis on submicron particle deposition from a forced laminar boundary layer flow on to an isothermal moving plate through similarity solutions. Only just, Selim *et al.* (2003) premeditated the effect of thermophoresis and surface mass transfer on mixed convection flow past a heated vertical flat permeable plate. The study of heat generation or absorption effects in moving fluids is important in view of quite a few physical problems such as fluids undergoing exothermic or endothermic chemical reactions. In addition, natural convection with heat generation can be applied to combustion modeling. In light of these applications, Moalem (1976) studied the effect of temperature dependent heat sources taking place in electrically heating on the heat transfer within a porous medium. Vajrevelu and Nayfeh (1992) reported on the hydromagnetic convection at a cone and a wedge in the presence of temperature dependent heat generation or absorption effects. Chamkha (1999) studied the effect of heat generation or absorption on hydromagnetic three-dimensional free convection flow over a vertical stretching surface. Rahman and Sattar (2006) studied the effect of heat generation or absorption on convective flow of a micropolar fluid past a continuously moving vertical porous plate in existence of a magnetic field. Very recently, Alam *et al.* (2007) studied the similarity Solutions for hydromagnetic free convective Heat and mass transfer flow along a semi-infinite permeable inclined flat plate with heat generation and thermophoresis. Therefore; the objective of this study is to consider the effects of

different parameters which are entering into the fluid flows in the presence of heat generation and thermophoresis on steady, laminar, hydromagnetic, two-dimensional flow with heat and mass transfer along a semi-infinite, permeable inclined flat surface.

## MATHEMATICAL FORMULATION

Regard as the steady, laminar, hydromagnetic united heat and mass transfer by natural convection flow along a continuously moving semi-infinite permeable plate that is inclined with an acute angle  $\alpha$  from the vertical. With  $x$  –axis deliberated along the plate, a magnetic field of uniform strength  $B_0$  is applied in the  $y$  direction which is normal to the flow direction. Fluid suction is imposed at the plate surface. A heat source is positioned within the flow to allow for probable heat generation effects. The fluid is assumed to be Newtonian, electrically conducting and heat generating. The temperature of the surface is held uniform at  $T_w$  which is higher than the ambient temperature  $T_\infty$ . The species concentration at the surface is maintained uniform at  $C_w$ , which is taken to be zero and that of the ambient fluid is assumed to be  $C_\infty$ . The effects of thermophoresis are being taken into account to help in the understanding of the mass deposition variation on the surface. We further assume that:

- The mass flux of particles is sufficiently small so that the main stream velocity and temperature fields are not affected by the thermophysical processes experienced by the relatively small number of particles
- The magnetic Reynolds number is assumed to be small so that the induced magnetic field is negligible in comparison to the applied magnetic field
- The fluid has constant kinematic viscosity and thermal diffusivity and that the Boussinesq approximation may be adopted for steady laminar flow
- The particle diffusivity is assumed to be constant and the concentration of particles is sufficiently dilute to assume that particle coagulation in the boundary layer is negligible
- Due to the boundary layer behavior the temperature gradient in the  $y$  direction is much superior than that in the  $x$  direction and hence only the thermophoretic velocity component which is normal to the surface is of significance, Under the above assumptions, the governing equations (Selim *et al.*, 2003; Chen (2004) for this problem can be written as:

Continuity equation:

$$\frac{\partial u}{\partial x} + \frac{\partial v}{\partial y} = 0 \quad (1)$$

Momentum equation:

$$u \frac{\partial u}{\partial x} + v \frac{\partial u}{\partial y} = \nu \frac{\partial^2 u}{\partial y^2} + g\beta(T - T_\infty)\cos\alpha - \frac{\sigma B_0^2 u^2}{\rho x} + \frac{\nu}{K}u + \frac{b}{K}u^2 \quad (2)$$

Energy equation:

$$u \frac{\partial T}{\partial x} + v \frac{\partial T}{\partial y} = \frac{\lambda_g}{\rho c_p} \frac{\partial^2 T}{\partial y^2} + \frac{Q_0}{\rho c_p} (T - T_\infty) + \frac{D_m K_t}{c_s c_p} \frac{\partial^2 C}{\partial y^2} \quad (3)$$

Diffusion equation:

$$u \frac{\partial C}{\partial x} + v \frac{\partial C}{\partial y} = D \frac{\partial^2 C}{\partial y^2} - \frac{\partial}{\partial y} (V_T C) \quad (4)$$

where,

- $u, v$  = The velocity components in the  $x$  and  $y$  directions respectively
- $\beta$  = The volumetric coefficient of thermal expansion
- $T, T_w$  and  $T_\infty$  = The temperature of the fluid inside the thermal boundary layer, the plate temperature and the fluid temperature in the free stream, respectively

while,

- $C, C_w$  and  $C_\infty$  = The corresponding concentrations
- $\nu$  = The kinematic viscosity
- $g$  = The acceleration due to gravity
- $\rho$  = The density of the fluid
- $\sigma$  = The electrical conductivity
- $B_0$  = The magnetic induction
- $\lambda_g$  = The thermal conductivity of fluid
- $c_p$  = The specific heat at constant pressure
- $K'$  = The Darcy permeability
- $D_m$  = Mass diffusivity
- $K_t$  = The thermal diffusion ratio
- $C_s$  = The concentration susceptibility
- $Q_0$  = The heat generation constant
- $D$  = The molecular diffusivity of the species concentration
- $V_T$  = The thermophoretic velocity

The appropriate boundary states of affairs for the above model are as follows:

$$\left. \begin{aligned} u = U_0, v = \pm v_w(x), T = T_w, C = C_w, \text{ at } y = 0 \\ u = 0, T = T_\infty, C = C_\infty \text{ as } y \rightarrow \infty \end{aligned} \right\} \quad (5)$$

where,  $U_0$  is the uniform plate velocity and  $v_w(x)$  represents the permeability of the porous surface where its sign indicates suction ( $> 0$ ) or blowing ( $< 0$ ). Here we lock up our attention to the suction of the fluid through the porous surface and for these we also consider that the transpiration function variable  $v_w(x)$  is

of the order of  $x^{-\frac{1}{2}}$ . The effect of thermophoresis is usually prescribed by means of an average velocity that a particle will acquire when exposed to a temperature gradient. For boundary layer analysis it is found that the temperature gradient along the plate is much minor than the temperature gradient normal to the surface, i.e.,  $\frac{\partial T}{\partial y} \gg \frac{\partial T}{\partial x}$ . So the component of thermophoretic velocity along the plate is trifling compared to the component of its normal to the surface. As a result, the thermophoretic velocity  $V_T$ , which appears in Eq. (4), can be written as:

$$V_T = -\kappa \nu \frac{\nabla T}{T_{ref}} = -\frac{\kappa \nu}{T_{ref}} \frac{\partial T}{\partial y} \quad (6)$$

where,  $\kappa$  is the thermophoretic coefficient which ranges in value from 0.2 to 1.2 as indicated by Batchelor and Shen (1985) and is defined from the theory of Talbot *et al.* (1980) by:

$$\kappa = \frac{2C_s(\frac{\lambda_g}{\lambda_p} + C_t Kn)[1 + Kn(C_1 + C_2 e^{-C_3/Kn})]}{(1 + 3C_m Kn)(1 + 2\lambda_g/\lambda_p + 2C_t Kn)} \quad (7)$$

where,  $C_1, C_2, C_3, C_m, C_s, C_t$  are constants,  $\lambda_g$  and  $\lambda_p$  are the thermal conductivities of the fluid and diffused particles, respectively and  $Kn$  is the Knudsen number. A thermophoretic parameter  $\tau$  can be defined (Mills *et al.*, 1984; Tsai, 1999) as follows:

$$\tau = -\frac{\kappa(T_w - T_\infty)}{T_{ref}} \quad (8)$$

In order to obtain similarity solution of the problem we introduce the following non-dimensional variables:

$$\eta = \sqrt{\frac{U_0}{2\nu x}}, \quad \psi = \sqrt{2\nu x} f(\eta), \quad \theta(\eta) = \frac{T - T_\infty}{T_w - T_\infty}, \quad \phi(\eta) = \frac{C}{C_\infty} \quad (9)$$

where,  $\psi$  is the stream function that satisfies the continuity Eq. (1). Since  $u = \frac{\partial \psi}{\partial y}$  and  $v = -\frac{\partial \psi}{\partial x}$  we have from Eq. (9):

$$u = U_0 f' \text{ and } v = \sqrt{\frac{\nu U_0}{2x}} (f - \eta f')$$

Here prime denotes the ordinary differentiation with respect to  $\eta$ . Now substituting Eq. (9) in Eq. (2) to (4) we get hold of the following ordinary differential equations which are locally similar:

$$f''' + ff'' + Gr\theta \cos\alpha -$$

$$Mf'^2 + \frac{2}{Da} f' + Fs f'^2 = 0 \tag{10}$$

$$J_s = -D\left(\frac{\partial C}{\partial y}\right)_{y=0} \tag{16}$$

$$\theta'' + Prf\theta' + PrQ\theta + Du Pr\phi'' = 0 \tag{11}$$

where,  $Re = \frac{U_0 2x}{\nu}$  is the local Reynolds number.

$$\phi'' + Sc(f - \tau\theta')\phi' - Sc\tau\phi\theta'' = 0 \tag{12}$$

### NUMERICAL COMPUTATION

The boundary conditions (5) then turn into:

$$\left. \begin{aligned} f = f_w, f' = 1, \theta = 1, \phi = 0 \text{ at } \eta = 0 \\ f' = 0, \theta = 0, \phi = 1 \text{ as } \eta \rightarrow \infty \end{aligned} \right\} \tag{13}$$

The set of nonlinear ordinary differential Eq. (10) to (12) with boundary conditions (13) have been solved numerically by applying Nachtsheim and Swigert (1965) shooting iteration technique (for detailed discussion of the method see Alam (2004), Maleque and Sattar (2005) and Alam *et al.* (2006) along with sixth order Runge-Kutta integration scheme. A step size of  $\Delta\eta = 0.001$  was selected to be satisfactory for a convergence criterion of  $10^{-6}$  in all cases. The value of  $\eta_\infty$  was found to each iteration loop by the statement  $\eta_\infty = \eta_\infty + \Delta\eta$ . The maximum value of  $\eta_\infty$  to each group of parameters  $M, Gr, Pr, Sc, Q, f_w, \tau$  and  $\alpha$  determined when the value of the unknown boundary conditions at  $\eta = 0$  not change to successful loop with error less than  $10^{-6}$ . In a shooting method, the missing (unspecified) initial condition at the initial point of the interval is assumed and the differential equation is then integrated numerically as an initial value problem to the terminal point. Comparing the calculated value of the dependent variable at the terminal point with its given value there then checks the accuracy of the assumed missing initial condition. If a difference exists, another value of missing initial condition must be assumed and the process is repeated. This process is continued until the agreement between the calculated and the given condition at the terminal point is within the specified degree of accuracy. For this type of iterative approach, one naturally inquires whether or not there is a systematic way of finding each succeeding (assumed) value of the missing initial condition. For a brief discussion of the Nachtsheim–Swigert shooting iteration technique, the readers may also consult the study of Rahman (2009) and Alam *et al.* (2006). Thus adopting this numerical technique, a computer program was set up for the solutions of the governing non-linear ordinary differential equations of our problem with a sixth order Runge–Kutta method of integration.

where,  $f_w = -v_w(x)\sqrt{\frac{2x}{\nu U_0}}$  is the dimensionless wall transfer coefficient such that  $f_w > 0$  indicates wall suction. The dimensionless parameters introduced in the above equations are defined as follows:

$$\begin{aligned} M = \frac{\sigma B_0^2 2x}{\rho U_0} &= \text{The local magnetic field parameter} \\ Gr = \frac{g\beta(T_w - T_\infty)2x}{U_0^2} &= \text{The local Grashof number} \\ Du = \frac{D_m K t}{C_s C_p \nu} \left(\frac{C_w - C_\infty}{T_w - T_\infty}\right) &= \text{The Dufour number} \\ Pr = \frac{\nu \rho C_p}{\lambda_g} &= \text{The Prandtl number} \\ Q = \frac{Q_0 2x}{\rho C_p U_0} &= \text{The local heat generation parameter} \\ Sc = \frac{\nu}{D} &= \text{The Schmidt number} \\ \tau = -\frac{\kappa(T_w - T_\infty)}{T_{ref}} &= \text{The thermophoretic parameter} \\ Da = \frac{K' U_0}{\nu x} &= \text{The modified Darcy number} \\ Fs = \frac{bx}{K'} &= \text{The modified Forchhemier number} \end{aligned}$$

The skin-friction coefficient, wall heat transfer coefficient (or local Nusselt number) and wall deposition flux (or the local Stanton number) are important physical parameters. These can be obtained from the following expressions:

$$Cf_x Re_x^{1/2} = \frac{\tau_w}{\rho U_0^2} = f''(0) \tag{14}$$

$$\tau_w = \mu \left(\frac{\partial u}{\partial x}\right)_{y=0} \tag{14}$$

$$Nu_x Re_x^{-1/2} = \frac{xq_w}{(T_w - T_\infty)\lambda_g} = -\frac{1}{2}\theta'(0) \tag{15}$$

$$q_w = -\lambda_g \left(\frac{\partial T}{\partial y}\right)_{y=0} \tag{15}$$

$$St_x Sc Re_x^{1/2} = -\frac{J_s}{U_0 C_\infty} = \phi'(0)$$

**Code verification:** Table 1 presents a comparison of the local Stanton number obtained in the present study and those obtained by Alam *et al.* (2007). It is clearly observed that very good agreement between the results exists. This provides the confidence in the present numerical method.

In order to verify the effect of the integration step size  $\Delta\eta$ , we tested the code with three different step sizes namely  $\Delta\eta = 0.001$ ,  $\Delta\eta = 0.002$   $\Delta\eta = 0.003$  and

Table 1: Comparison of local Stanton number with those of Alam *et al.* (2007) for  $Sc = 0.60, Pr = 0.70, \alpha = 30^\circ, Gr = 6.0, M = 0.5, Q = 0.5$  and  $Fs = Du = Da = 0$

$\tau$	$f_w$	Alam <i>et al.</i> (2007)	Present work
0.01	1.0	1.02290102	1.02746696
0.01	0.5	0.83816211	0.84005565
0.01	0.0	0.67509657	0.67309633
0.10	1.0	1.02688968	1.03157217
0.10	0.5	0.84261992	0.84461581
0.10	0.0	0.67976419	0.67788221
1.00	1.0	1.06465091	1.07023610
1.00	0.5	0.88513527	0.88803701
1.00	0.0	0.72507750	0.72400194

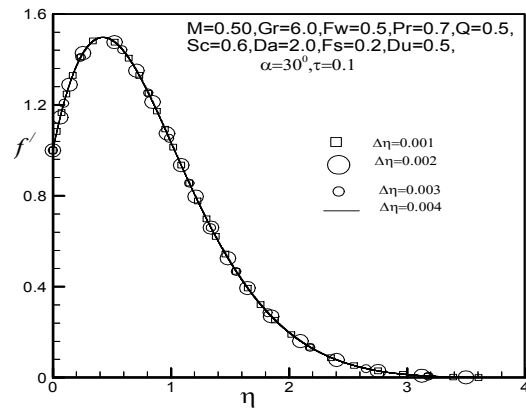
$\Delta\eta = 0.004$ . In each case we found excellent agreement among the results. Figure 1a-c, respectively; show the velocity, the microrotation and the temperature profiles for the three step sizes. The results for the three different step sizes are graphically indistinguishable. It was found that  $\Delta\eta = 0.002$  provided sufficiently accurate results and further refinement of the grid size was therefore not warranted.

**RESULTS AND DISCUSSION**

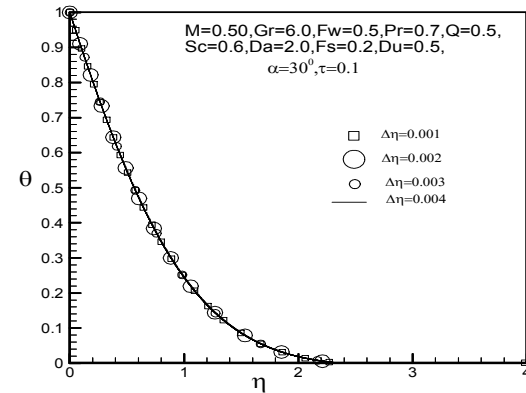
Numerical calculations have been carried out for different values of  $M, Q, \alpha, Pr, \tau, Da, Du, Fs$  and  $f_w$  and for fixed values of  $Gr$  and  $Sc$ . The value of  $Pr$  is taken to be 0.70 which correspond physically to air. Due to free convection problem positive large value of  $Gr = 6$  is taken which correspond to a cooling problem that is generally encountered in nuclear engineering in connection with cooling of reactor. The values of Schmidt number  $Sc$  are taken for water-vapour ( $Sc = 0.60$ ).

Figure 2a-c present typical profiles for the velocity, temperature and concentration for various values of the magnetic field parameter  $M$ , respectively for a physical situation with heat generation and thermophoretic effect. The presence of a magnetic field normal to the flow in an electrically conducting fluid introduces a Lorentz force which acts against the flow. This resistive force tends to slow down the flow and hence the fluid velocity decreases with the increase of the magnetic field parameter as observed in Fig. 2a. From Fig. 2b we see that the temperature profiles enhance with the increase of the magnetic field parameter, which implies that the applied magnetic field tends to heat the fluid and thus reduces the heat transfer from the wall. In Fig. 2c, the effect of an applied magnetic field is found to decrease the concentration profiles and hence increase the concentration boundary layer.

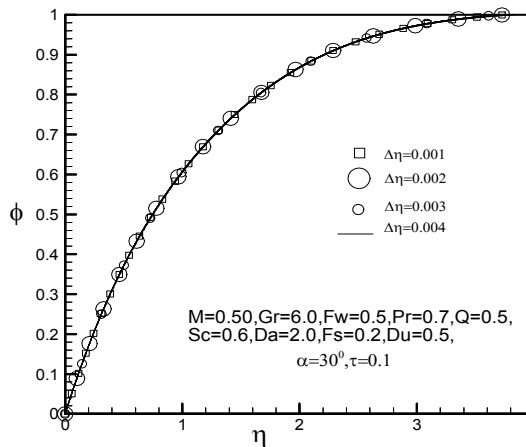
In this regards the skin-friction coefficients  $Cf_x Re_x^{1/2}$  are 3.2537, 2.5233, 1.9983, 1.5912, 1.2586 for the corresponding values of  $M = 0.0, 0.5, 1.0, 1.5, 2.0$  respectively whereas the values of wall heat transfer (or local Nusselt number)  $Nu_x Re_x^{-1/2}$  are 0.5236, 0.4963, 0.4754, 0.4584, 0.4441 and also the values of wall



(a)



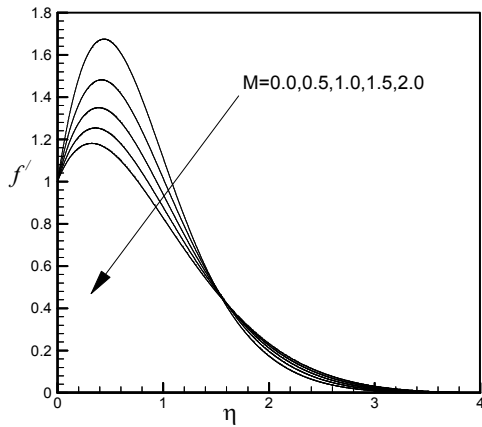
(b)



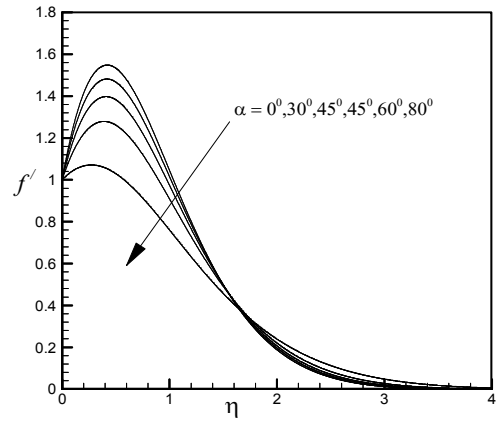
(c)

Fig. 1: (a) Velocity, (b) temperature and (c) concentration profiles for different values of  $\Delta\eta$

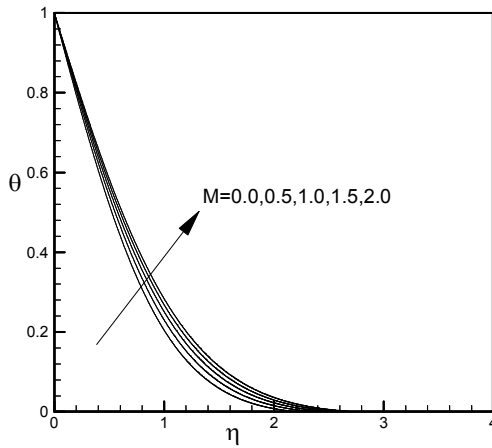
deposition flux (or the local Stanton number)  $St_x Sc Re_x^{1/2}$  are 0.9140, 0.8783, 0.8516, 0.8304, 0.8131. From these values it clear that the skin-friction coefficient, local Nusselt number and the local Stanton



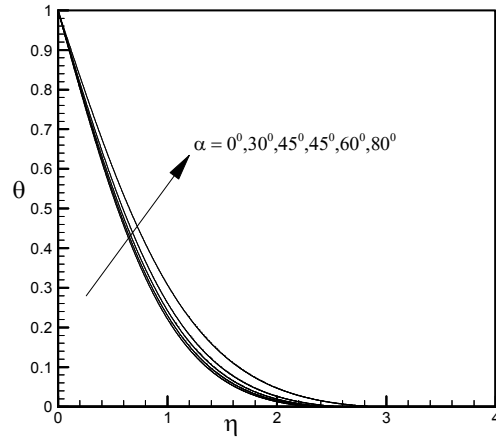
(a)



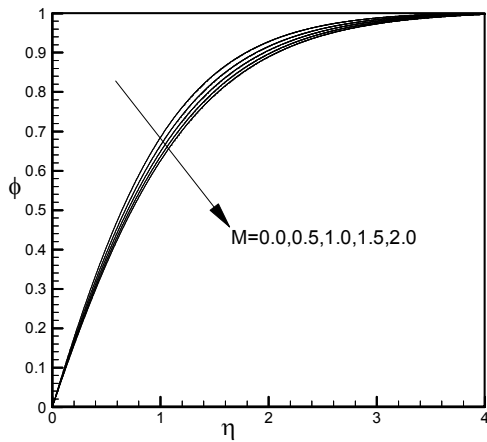
(a)



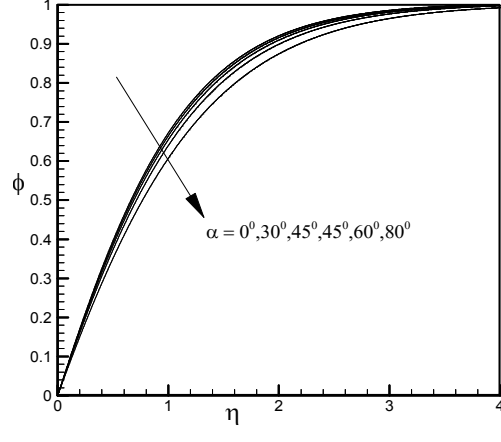
(b)



(b)



(c)



(c)

Fig. 2: Variations of non-dimensional (a) velocity, (b) temperature and (c) concentration profiles for different values of magnetic field parameter  $M$

Fig. 3: Variations of non-dimensional (a) velocity (b) temperature and (c) concentration profiles for different values of angle of inclination  $\alpha$

number are decreases with the increase of Magnetic field parameter.

The effect of the angle of inclination  $\alpha$  on the velocity field is shown in Fig. 3a. From this figure we

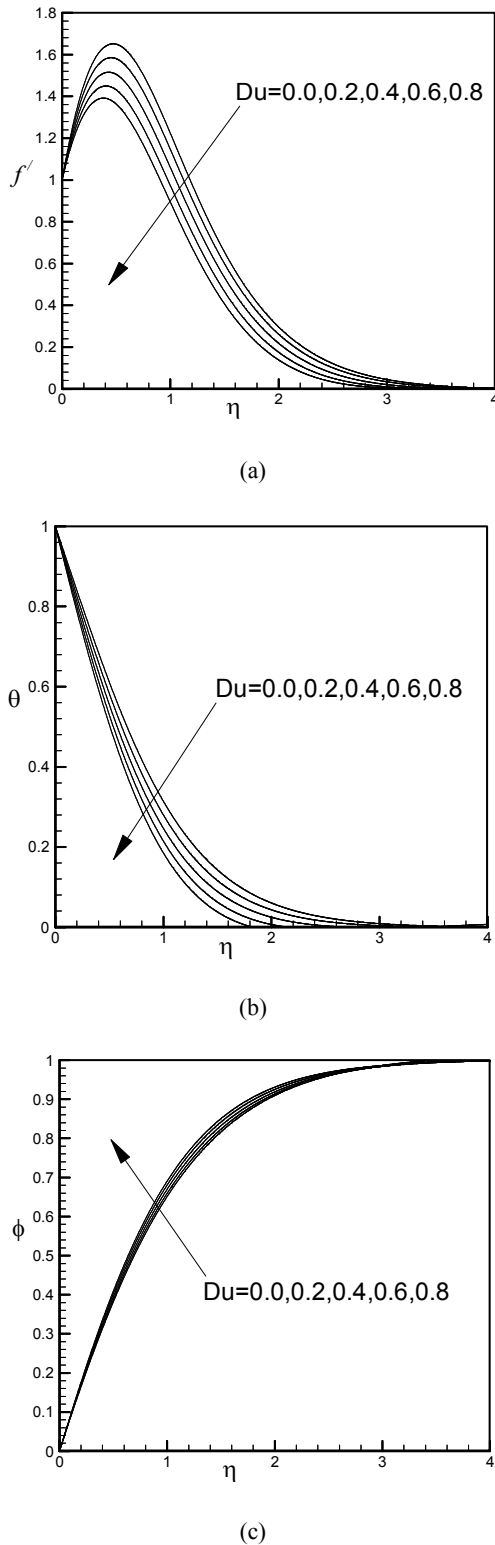


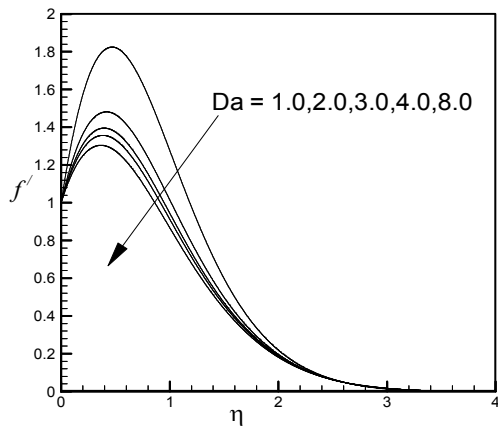
Fig. 4: Variations of non-dimensional (a) velocity (b) temperature and (c) concentration profiles for different values of dufour number  $Du$

see that the velocity decreases with the increase of  $\alpha$ . As  $\alpha$  increases, the effect of the buoyancy force

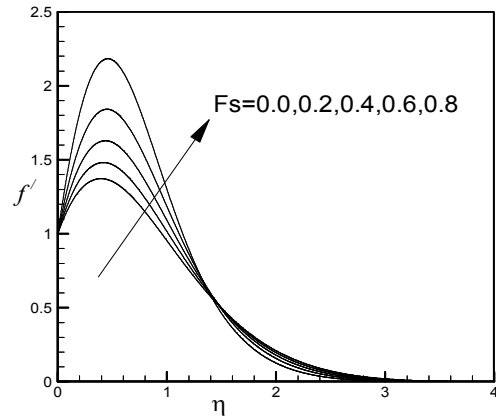
decreases because of the multiplication factor  $\cos \alpha$  and the velocities decrease. Figure 3b shows the effect of  $\alpha$  in the temperature profiles. We observe that the angle of inclination  $\alpha$  strongly affects the temperature near the plate surface. Away from the plate, however, the temperature profiles are minimally affected by the angle of inclination and it is increases with the increase of  $\alpha$ . Figure 3c shows that as the angle of inclination increases, the concentration profile go up. In this gaze at, the skin-friction coefficients, local Nusselt number and the local Stanton number are investigated where the values of the skin-friction coefficients are 2.8582, 2.5233, 2.1105, 1.5439, 0.5456 whereas the local Nusselt numbers are 0.5060, 0.4963, 0.4835, 0.4640, 0.4215 and also the local Stanton numbers are 0.8914, 0.8783, 0.8614, 0.8361, 0.7838 for different values of  $\alpha = 0^\circ, 30^\circ, 45^\circ, 60^\circ, 80^\circ$  respectively. From these investigations it can be articulate that the skin-friction coefficients (80.91%), local Nusselt number (4.28%) and the local Stanton number (9.59%) are decreases with the increases of  $\alpha$  from  $0^\circ$  to  $80^\circ$ .

In Fig. 4 we plotted the dimensionless velocity, temperature and concentration profiles showing the effects of the Dufour number  $Du$ . It can be seen that the velocity  $f'$  and the temperature profile  $\theta$  decreases while the concentration profile  $\phi$  increases, when the Dufour number increases. The effect of Dufour number is stronger near the surface of the plate. As the Dufour number increases, viscous forces tend to suppress the buoyancy forces and cause the velocity in the hydrodynamic boundary layer to decrease. It is also observed that the maximum values of the velocity are 1.6514, 1.5850, 1.5154, 1.4496 and 1.3916 for  $Du = 0.0, 0.2, 0.4, 0.6$  and  $0.8$  respectively and occur at  $\eta = 0.47, 0.45, 0.428, 0.404$  and  $0.38$ , respectively. It is observed that the maximum velocity decreases by 15.73% when  $Du$  increases from 0.0 to 0.8. Figure 4b shows the effect of Dufour number on the temperature profiles. This figure reveals that the effects of the Dufour number on the hydrodynamic boundary layer are analogous to those found in the thermal boundary layer. Furthermore the maximum values of the temperature are observed to be 1.0 for all increasing values of Dufour number occurs at  $\eta = 0$ . Figure 4c is evidence for the effect of Dufour number on the concentration profiles. The maximum values of the concentration are scrutinized to be approximately close to 1 for all values of the Dufour number. The values of the skin-friction coefficient and the local Stanton number are decreases at the rate of 25.36 and 5.63%, respectively while the local Nusselt number increases at the rate of 6% when  $Du$  increases from 0.0 to 0.8.

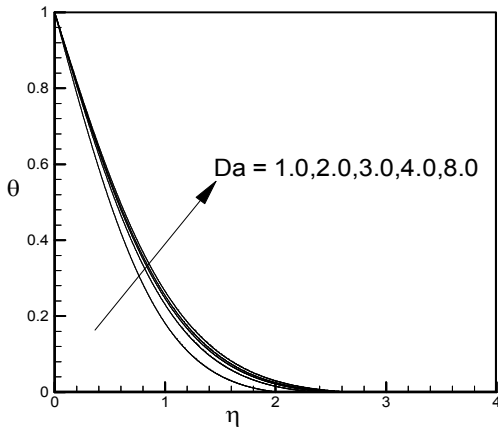
The effect of the local Darcy parameter  $Da$  on the velocity field is shown in the Figure 5a. From this figure we watch that velocity profiles decrease with the increase of  $Da$ . Figure 5b shows that temperature increases with the increase of Darcy parameter  $Da$ . The



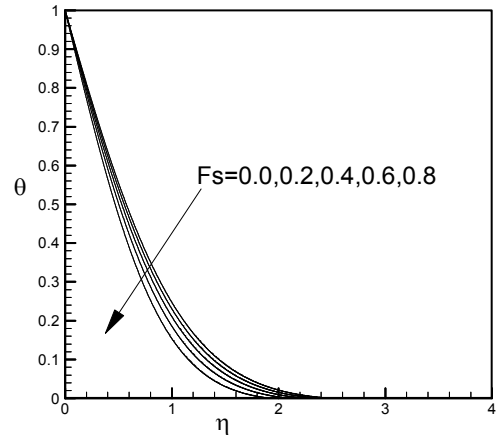
(a)



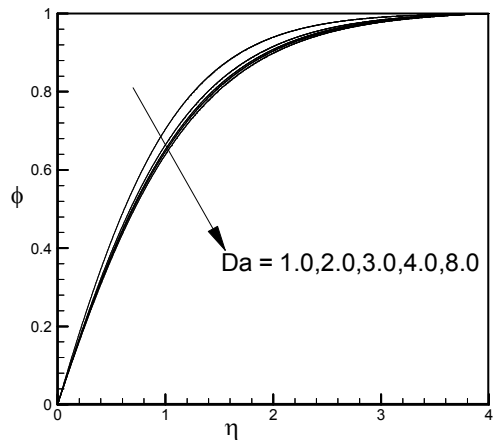
(a)



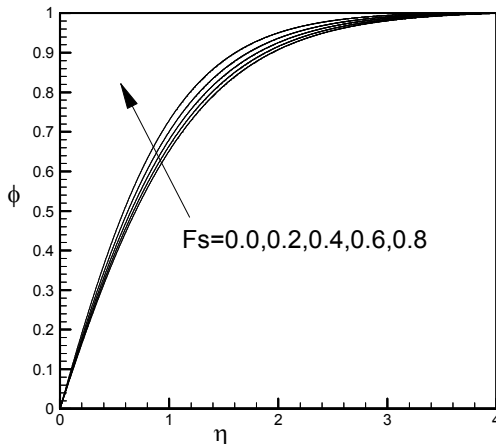
(b)



(b)



(c)



(c)

Fig. 5: Variations of non-dimensional (a) velocity (b) temperature and (c) concentration profiles for different values of modified Darcy parameter  $Da$

Fig. 6: Variations of non-dimensional (a) velocity (b) temperature and (c) concentration profiles for different values of forchhemier number  $Fs$

effect of  $Da$  on the concentration profiles is shown in Fig. 5c. From this figure we see that concentration

profiles decreases with the increase of Darcy parameter. As  $Da$  increases, the resistance to the flow also

decreases, which means that concentration field approximates more far away to the equivalent conductive state. It is watched that the maximum values of the velocity are 1.8251, 1.4818, 1.3956, 1.3573 and 1.3044 for  $Da = 1, 2, 3, 4$  and  $8$ , respectively and occur at  $\eta = 0.47, 0.45, 0.428, 0.404$  and  $0.380$  respectively. It is also found that the maximum velocity decreases by 28.53% as  $Da$  increases from 1.0 to 8.0. The skin-friction coefficients, local Nusselt number and the local Stanton number are decreases by 51.31, 4.6, 10.39%, respectively as  $Da$  increases from 1 to 8.

Figure 6a – c respectively, shows the velocity, temperature and concentration profiles for different values of Modified Forchheimer number  $F_s$ . From Fig. 6a we note that velocity increases with the increase of Forchheimer number  $F_s$ . This effect is stronger near the surface of the plate. It is also observed that away from the plate ( $\eta \geq 1.2$ ) this profiles overlap. It is carefully experimented that the maximum values of the velocity are 1.3728, 1.4818, 1.6290, 1.8420, 2.1834 for  $F_s = 0.0, 0.2, 0.4, 0.8$ , respectively and take place at  $\eta = 0.394, 0.416, 0.434, 0.450, 0.458$ , respectively. From Fig. 6b we see that temperature decreases with the increase of Forchheimer number  $F_s$ . Figure 6c shows that as the Forchheimer number increases, the thermal boundary layer thickens and the concentration rise. The skin-friction coefficients, local Nusselt number and the local Stanton number are increases by 145, 5.03, 12%, respectively as  $F_s$  increases from 0.0 to 0.80. We can depicted from this result that the effect of Forchheimer number on the skin-friction coefficient is greater than the effect of other parameters.

Figure 7a – c, respectively, shows the velocity, temperature and concentration profiles for different values of suction parameter  $f_w$ . From Fig. 7a we note that the velocity decreases with the increase of the suction parameter indicating that the suction tends to retard the convective motion of the fluid. It can also be seen that for cooling of the plate the velocity profiles decrease monotonically with increase of suction parameter indicating the usual fact that suction stabilizes the boundary layer growth. This effect is stronger near the surface of the plate. From Fig. 3b we see that temperature decreases with the increase of the suction parameter. As we move away from the plate, the effect of  $f_w$  becomes more pronounced. Figure 3c reveals that the concentration in the thermal boundary layer increases with the increase of suction parameter. This is due to the fact that suction tends to speed up the velocity field, which in turn increase the heat transfer. This is manifested with higher concentration in the thermal boundary layer. The skin-friction coefficients decreases by 88.18% whereas local Nusselt number and the local Stanton number are increases by 5 and 53.90% respectively when  $f_w$  increases from 0 to 2.

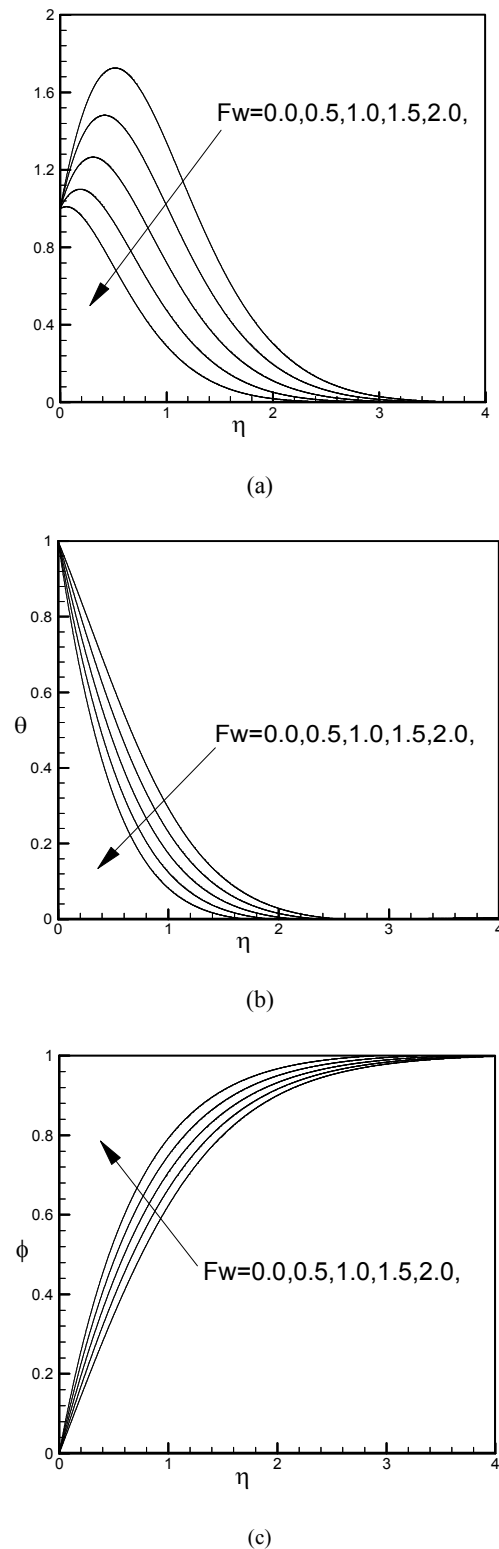
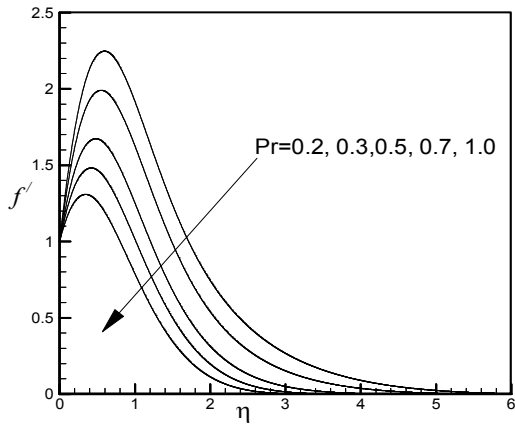
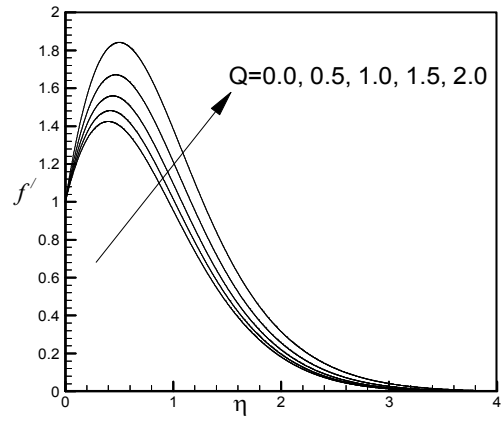


Fig. 7: Variations of non-dimensional (a) velocity (b) temperature and (c) concentration profiles for different values of suction parameter  $f_w$

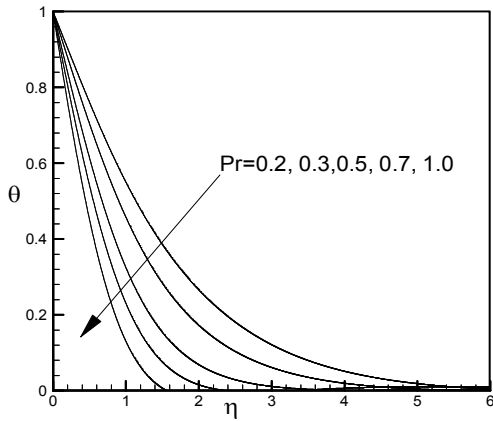
Figure 8a – c shows the velocity profiles, temperature profiles and concentration profiles for



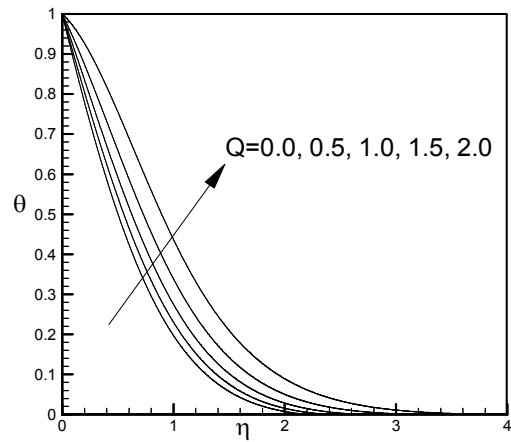
(a)



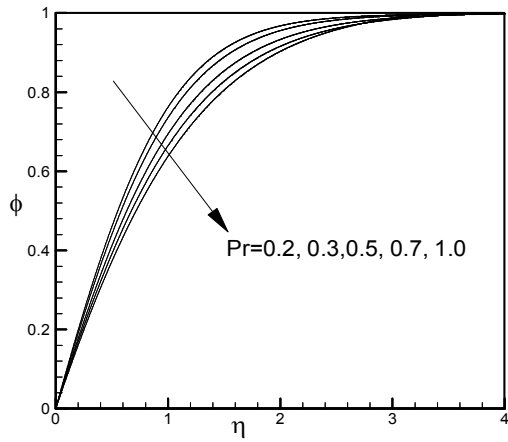
(a)



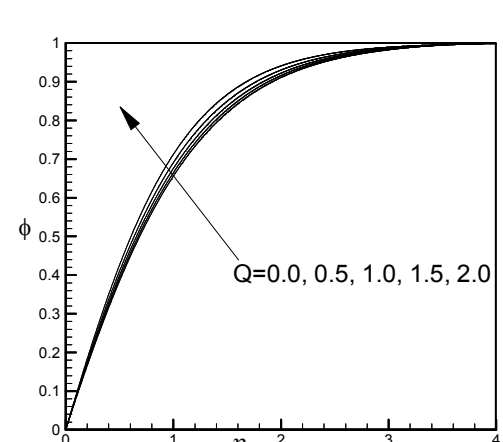
(b)



(b)



(c)



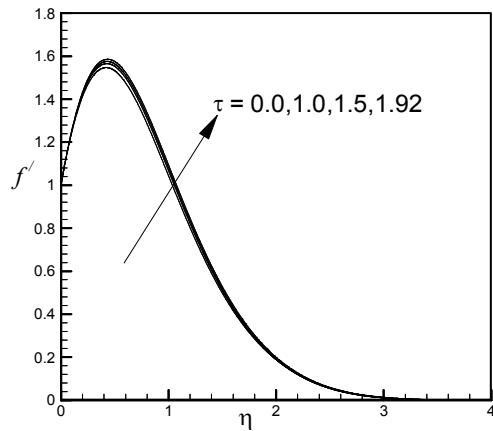
(c)

Fig. 8: Variations of non-dimensional (a) velocity (b) temperature and (c) concentration profiles for different values of prandtl number  $Pr$

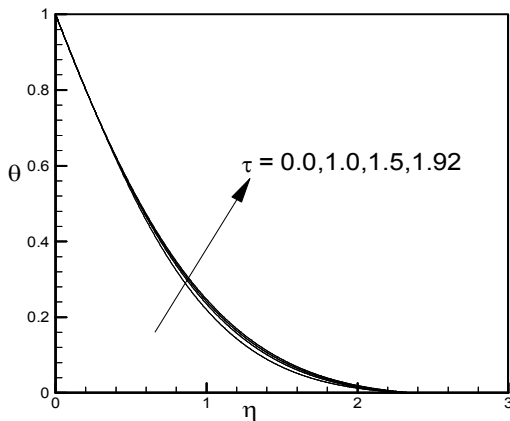
Fig. 9: Variations of non-dimensional (a) velocity (b) temperature and (c) concentration profiles for different values of heat generation parameter  $Q$

different values of Prandtl number  $Pr$ . The effects of Prandtl number into this fluid flow are sensitive. As the Prandtl number increases, fluid forces tend to suppress

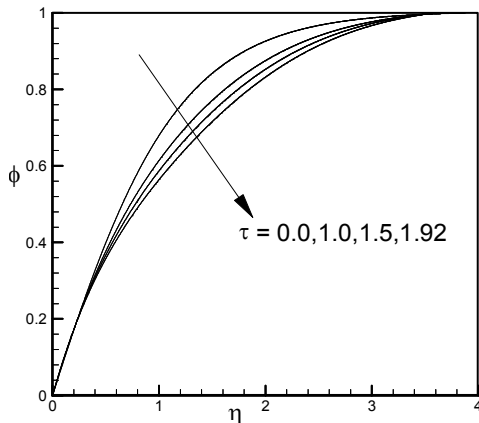
the buoyancy forces and cause the velocity in the hydrodynamic boundary layer to decrease. It is also observed that the maximum values of the velocity are



(a)



(b)



(c)

Fig. 10: Variations of non-dimensional (a) velocity (b) temperature and (c) concentration profiles for different values of thermophoretic parameter  $\tau$  and in this case the angle of inclination  $\alpha = 0^\circ$

2.2472, 1.9907, 1.6732, 1.4817, 1.3086 for  $Pr = 0.2, 0.3, 0.5, 0.7, 1.0$ , respectively and occur at  $\eta =$

0.592, 0.548, 0.476, 0.416, 0.342, respectively. It is seen that the maximum velocity decreases by 41.77% when  $Pr$  increases from 0.2 to 1. Figure 8b-c shows the decreasing affect on temperature profiles and concentration profiles respectively as Prandtl number increases. The skin-friction coefficients and the local Stanton number are decreases by 56.25 and 18.98% respectively whereas local Nusselt number is increases by 9.15% when  $Pr$  increases from 0.2 to 1.

Figure 9a-c depict the influence of the dimensionless heat generation parameter  $Q$  on the fluid velocity, temperature and concentration profiles respectively. It is seen from Figure 9a that when the heat is generated the buoyancy force increases, which induces the flow rate to increase giving, rise to the increase in the velocity profiles. It is also investigated that the maximum values of the velocity are 1.4243, 1.4818, 1.5595, 1.6710, 1.8417 for  $Q = 0.0, 0.5, 1.0, 1.5, 2.0$ , respectively and occur at  $\eta = 0.396, 0.416, 0.438, 0.466, 0.500$  respectively. It is also calculated that maximum velocity increases at the rate of 29.31% as  $Q$  increases from 0 to 2. From Figure 9b, we observe that when the value of the heat generation parameter  $Q$  increases, the temperature distribution also increases significantly which implies that owing to the presence of a heat source, the thermal state of the fluid increases causing the thermal boundary layer to increase. On the other hand, from Figure 9c we see that the concentration profiles increase while the concentration boundary layer decreases as the heat generation parameter  $Q$  increases. The skin-friction coefficients and the local Stanton number are increases by 53.03 and 7.84% respectively whereas local Nusselt number decreases by 26.15%, when  $Q$  increases from 0 to 2.

Figure 10a-c illustrate the manipulation of the dimensionless thermophoretic parameter,  $\tau$  in the fluid flow velocity, temperature and concentration profiles respectively for the case of  $\alpha = 0^\circ$ . The velocity and the temperature profiles are increase whereas the concentration profiles are lessen as the rises of thermophoretic parameter considered  $\tau = 0.0, 1.0, 1.5, 1.952$ . The effect of thermophoretic parameter in this case is very sensitive when  $\tau > 1.952$  and found that the velocity, temperature and concentration are in this case decreases rapidly. The skin-friction coefficients, local Nusselt number and the local Stanton number are increases by 3.71, 1.10 and 10.05%, respectively when  $Q$  increases from 0 to 1.952.

### NOMENCLATURE

- $B_0$  = Magnetic induction, ( $Wb\ m^{-2}$ )
- $C_f$  = Skin-friction coefficient
- $c_p$  = Specific heat at constant pressure, ( $J\ kg^{-1}K^{-1}$ )
- $f$  = Dimensionless stream function

$g_0$  = Acceleration due to gravity, ( $m s^{-2}$ )  
 $C$  = Dimensionless microrotation  
 $h(x)$  = Local heat transfer coefficient  
 $M$  = Magnetic field parameter  
 $M_x$  = Dimensionless couple stress  
 $M_w$  = Couple stress at the plate, ( $Pa m$ )  
 $Nu_x$  = Local Nusselt number  
 $Pr$  = Prandtl number  
 $Q$  = Heat generation parameter  
 $Da$  = The modified Darcy parameter  
 $FS$  = The modified Forchheimer number  
 $K'$  = The Darcy permeability  
 $q_w$  = Surface heat flux, ( $W m^{-2}$ )  
 $T$  = Temperature of the fluid within boundary layer, ( $K$ )  
 $T_w$  = Temperature at the surface of the plate, ( $K$ )  
 $T_\infty$  = Temperature of the ambient fluid, ( $K$ )  
 $u$  = Velocity along x -axis, ( $m s^{-1}$ )  
 $v$  = Velocity along y -axis, ( $m s^{-1}$ )  
 $x$  = Coordinate along the plate, ( $m$ )  
 $y$  = Coordinate normal to the plate, ( $m$ )

#### Greek symbols:

$\alpha$  = Angle of inclination (rad)  
 $\beta$  = Coefficient of volume expansion  
 $\rho$  = Density of the fluid, ( $kg m^{-3}$ )  
 $\mu$  = Coefficient of dynamic viscosity, ( $Pa s$ )  
 $\nu$  = Apparent kinematic viscosity, ( $m^2 s^{-1}$ )  
 $\sigma_0$  = Magnetic permeability, ( $N A^{-2}$ )  
 $\psi$  = Stream function, ( $m^2 s^{-1}$ )  
 $\kappa$  = Thermal conductivity of the fluid, ( $W m^{-1} K^{-1}$ )  
 $\eta$  = Similarity parameter  
 $\tau_w$  = Shear stress, ( $Pa$ )  
 $\theta$  = Dimensionless temperature  
 $\Delta\eta$  = Step size  
 $\phi$  = Dimensionless concentration

#### Subscripts

$w$  = Surface condition  
 $\infty$  = Conditions far away from the surface

### CONCLUSION

In this study we have studied numerically the effects of thermophoresis and heat generation on hydromagnetic free convection heat and mass transfer flow past a continuously moving semi-infinite inclined permeable porous plate. The particular conclusions drawn from this study can be listed as follows:

- In the presence of a magnetic field, the fluid velocity is found to be decreased, associated with a reduction in the velocity gradient at the wall and thus the local skin-friction coefficient decreases. Also, the applied magnetic field tends to increase the wall temperature gradient and decrease the

concentration gradient, which yield a decrease the local Nusselt number and the local Stanton number. For this study the same results are found by the effects of angle of inclination, Dufour number modified Darcy parameter and the modified Forchheimer number.

- For a suction parameter, the velocity, temperature profiles are decreases while the skin-friction coefficient and the concentration are increases.
- For a fixed magnetic field parameter, the local skin-friction was found to decrease whereas the local Nusselt and Stanton number was found to increase when the value of wall suction increases.
- As the heat generation parameter increases, both the velocity and thermal boundary layer increases whereas concentration boundary layer decreases.
- The effects of Prandtl number and heat generation parameter to this study are inversely proportional to each other.
- As the thermophoretic parameter  $\tau$  increases up to 1.92, the surface mass flux also increases and velocity is dramatically decline when  $\eta \geq 0.5$ .

Finally it is hoped that the present study can be used as a vehicle for understanding the thermophoresis particle deposition on heat and mass transfer produced in steady, laminar boundary-layer flow past an inclined permeable surface in the presence of a magnetic field and heat generation.

### REFERENCES

- Alam, M.S., 2004. Thermal-diffusion and diffusion-thermo effects on magnetohydrodynamics heat and mass transfer. M.Phil. Thesis, BUET, Dhaka, Bangladesh.
- Alam, M.S., M.M. Rahman and M.A. Samad, 2006. Numerical study of the combined free-forced convection and mass transfer flow past: A vertical porous plate in a porous medium with heat generation and thermal diffusion. Nonlinear Anal. Model. Control, 11(4): 331-343.
- Alam, M.S., M.M. Rahman and M.A. Sattar, 2007. Similarity solutions for hydromagnetic free convective heat and mass transfer flow along a semi-infinite permeable inclined flat plate with heat generation and thermophoresis. Nonlinear Anal. Model. Control, 12(4): 433-445.
- Batchelor, G.K. and C. Shen, 1985. Thermophoretic deposition of particles in gas flowing over cold surface. J. Colloid Interf. Sci., 107: 21-37.
- Chamkha, A.J., 1999. Hydromagnetic three-dimensional free convection on a vertical stretching surface with heat generation or absorption. Int. J. Heat Fluid Fl., 20: 84-92.

- Chen, C.H., 2004. Heat and mass transfer in MHD flow by natural convection from a permeable inclined surface with variable wall temperature and concentration. *Acta Mech.*, 172: 219-235.
- Chiou, M.C. and J.W. Cleaver, 1996. Effect of thermophoresis on submicron particle deposition from a laminar forced convection boundary layer flow on to an isothermal cylinder. *J. Aerosol Sci.*, 27: 1155-1167.
- Epstein, M., G.M. Hauser and R.E. Henry, 1985. Thermophoretic deposition of particles in natural convection flow from a vertical plate. *J. Heat Tran.*, 107: 272-276.
- Garg, V.K. and S. Jayaraj, 1988. Thermophoresis of aerosol particles in laminar flow over inclined plates. *Int. J. Heat Mass Tran.*, 31: 875-890.
- Goren, S.L., 1977. Thermophoresis of aerosol particles in laminar boundary layer on flat plate. *J. Colloid Interf. Sci.*, 61: 77-85.
- Homsy, G.M., F.T. Geyling and K.L. Walker, 1981. Blasius series for thermophoretic deposition of small particles. *J. Colloid Interf. Sci.*, 83: 495-501.
- Jia, G., J.W. Cipolla and Y. Yener, 1992. Thermophoresis of a radiating aerosol in laminar boundary layer flow. *J. Thermophys. Heat Tran.*, 6: 476-482.
- Kennard, E.H., 1938. *Kinetic Theory of Gases*. McGraw Hill, New York.
- Kim, Y.J., 2004. Heat and mass transfer in MHD micropolar flow over a vertical moving porous plate in a porous medium. *Transport Porous Med.*, 56(1): 17-37.
- Maleque, K.A. and M.A. Sattar, 2005. The effects of variable properties and hall current on steady MHD laminar convective fluid flow due to a porous rotating disk. *Int. J. Heat Mass Tran.*, 48: 4963-4972.
- Mills, A.F., X. Hang and F. Ayazi, 1984. The effect of wall suction and thermo-phoresis on aerosol-particle deposition from a laminar boundary layer on a flat plate. *Int. J. Heat. Mass Tran.*, 27: 1110-1114.
- Moalem, D., 1976. Steady state heat transfer with porous medium with temperature dependent heat generation. *Int. J. Heat Mass Tran.*, 19: 529-537.
- Nachtsheim, P.R. and P. Swigert, 1965. Satisfaction of the Asymptotic Boundary Conditions in Numerical Solution of the System of Non-Linear Equations of Boundary Layer Type. NASA TND-3004, pp: 1-37.
- Rahman, M., 2009. Convective flows of micropolar fluids from radiate isothermal porous surfaces with viscous dissipation and joule heating. *Comm. Nonlinear Sci.*, 14: 3018-3030.
- Rahman, M.M. and M.A. Sattar, 2006. Magnetohydrodynamic convective flow of a micropolar fluid past a continuously moving vertical porous plate in the presence of heat generation /absorption. *ASME J. Heat Tran.*, 128: 142-152.
- Raptis, A. and N.G. Kafoussias, 1982. Magnetohydrodynamic free convection flow and mass transfer through porous medium bounded by an infinite vertical porous plate with constant heat flux. *Can. J. Phys.*, 60(12): 1725-1729.
- Selim, A., M.A. Hossain and D.A.S. Rees, 2003. The effect of surface mass transfer on mixed convection flow past a heated vertical flat permeable plate with thermophoresis. *Int. J. Therm. Sci.*, 42: 973-982.
- Talbot, L., R.K. Cheng, A.W. Schefer and D.R. Wills, 1980. Thermophoresis of particles in a heated boundary layer. *J. Fluid Mech.*, 101: 737-758.
- Tsai, R., 1999. A simple approach for evaluating the effect of wall suction and thermophoresis on aerosol particle deposition from a laminar flow over a flat plate. *Int. Comm. Heat Mass Tran.*, 26: 249-257.
- Vajrevelu, K. and J. Nayfeh, 1992. Hydromagnetic convection at a cone and a wedge. *Int. Comm. Heat Mass Tran.*, 19: 701-710.